

## SPECIFIC AIMS

Many health problems result from, or depend on, dysregulation of energy metabolism. For example, aggressive cancer cells shunt carbon away from aerobic respiration toward fermentation products and biomass. Three master regulators of carbon fate are conserved from yeast to man: AMP Activated Protein Kinase complex (AMPK), Protein Kinase A complex (PKA), and Target of Rapamycin complex (TOR). The long term goal of this project is to understand how the responsibility for carbon fate is divided among these three master regulators and the transcription factors (TFs) downstream of them in mammalian cells. In this application, we will study the regulation of carbon fate by AMPK and PKA in the model yeast *Saccharomyces cerevisiae*. The choice of AMPK and PKA is dictated by the need to keep the scope of the application reasonable and by evidence suggesting that AMPK and PKA may be more important than TOR in regulating energy metabolism and carbon fate.<sup>1</sup> The choice of *S. cerevisiae* was dictated by its tractability for the types of studies we propose, the remarkable conservation of the AMPK and PKA systems, and the depth of existing knowledge about how *cerevisiae* regulates energy metabolism and carbon fate. Quite a few of the DNA-binding TFs that serve as end effectors AMPK and PKA are known, but the mapping from TF to metabolic pathway is strikingly many-to-many: Each TF regulates genes encoding enzymes in several pathways and each pathway is regulated by several TFs. In each pathway, some genes are regulated by a single known TF, some by several, and some by none. One outcome of this proposal will be significant progress in understanding how responsibility for the regulation of carbon fate is divided among these TFs.

**Aim 1** Elucidate the influence of AMPK and PKA on gene expression and carbon fate.

Aim 1 will answer questions such as: How sensitive are gene regulation and carbon fate to changes in the activity levels of PKA and AMPK? What is the logic by which PKA and AMPK interact to influence carbon fate? Is it possible to decouple aerobic versus anaerobic metabolism from slow vs. fast growth, at least temporarily, by independently manipulating PKA and AMPK activity?

**Aim 2** Quantify the role of each effector TF in mediating the influence of AMPK and PKA on gene expression and on carbon fate.

Aim 2 parallels Aim 1 and answers similar questions at the level of downstream TFs.

**Aim 3** Build a quantitative model linking PKA and AMPK to metabolic outcomes via effector TFs.

When regulatory factors push in opposite directions, as do AMPK and PKA, a quantitative model is needed to predict the net impact of interventions on them and their downstream effectors. We will build such a model in the hope of providing insights or methods that could lead to therapeutic intervention.

Although the term “master regulator” is commonly used, “executive regulator” may be more apt. If the cell were an automobile company, AMPK and PKA would be vice presidents in charge of strategic direction. We know some of the middle managers that implement their decisions in light of current conditions and we know some of the foremen who direct the enzymatic line workers. But the chain of command is not a tree-like organization chart. Different foremen direct overlapping sets of workers on the same team, and each foreman directs members of several teams. When a strategic decision is made (analogous to “make fewer SUVs and more small cars”) communications go up and down the web of command. The aim of this project is to begin decoding that chatter. We are particularly interested in which foremen actually influence the short-term ratio of outputs in any given situation, and to what extent they do so. In the long run, we would also like to know what the other foremen are doing and in what situations their efforts become critical to implementing a particular strategy or to surviving its consequences.

## SIGNIFICANCE

Both yeast and animal cells regulate the balance among three fates to which carbon from glucose can be directed: aerobic energy generation (respiration), anaerobic energy generation (fermentation), or biomass formation. Most animal cells generate energy by respiration and grow slowly, but both yeast and fast-growing cancer cells shunt carbon to fermentation and biomass.

Conserved pathways regulate carbon fate Many of the mechanisms by which carbon fate is regulated are conserved from yeast to man, including major pathways involving AMPK and PKA. The heterotrimeric structure of AMPK, consisting of two regulatory subunits and one catalytic unit, is conserved,<sup>2</sup> as is the heterotetrameric structure of PKA, consisting of two regulatory and two catalytic subunits.<sup>3</sup> Many components the signaling networks associated with AMPK and PKA are also conserved. For example, the human AMP kinase LKB1 (a tumor suppressor gene associated with Peutz–Jeghers syndrome) can stand in for all three AMPK kinases in yeast. Conversely Tos3, one of three yeast AMPK kinases, activates mammalian AMPK by phosphorylating it on the residue orthologous to the residue it phosphorylates in yeast.<sup>4</sup> In both humans and yeast, PKA is activated by cyclic AMP (cAMP), the concentration of which is influenced by the balance cAMP synthesis catalyzed by adenylyl cyclase and cAMP degradation catalyzed by phosphodiesterases. Yeast Ras1 and Ras2, orthologs of the RAS protooncogene,<sup>3</sup> stimulate adenylyl cyclase.

Major roles in human health and disease AMPK and PKA play significant roles in human health and disease through their effects on energy metabolism and proliferation. As noted, rapidly growing cancer cells shunt carbon toward fermentation and biomass. Inhibiting fermentation by either genetic or pharmacological means has been shown to counteract growth of cancer cells both *in vitro* and *in vivo*, as has reactivation of oxidative phosphorylation.<sup>5</sup> In another example, Human AMPK activity is modulated by drugs used to treat type 2 diabetes (including metformin<sup>6</sup> and thiazolidinediones<sup>7</sup>), and by resveratrol,<sup>8</sup> which reportedly reduces obesity and insulin resistance and may extend lifespan.

## INNOVATION

There have been many studies of the genes that go up and down when the yeast AMPK or PKA pathways are affected by changing carbon sources or by genetic manipulation.<sup>1,14,15</sup> There have also been studies of metabolic fluxes when carbon sources are changed.<sup>16</sup> But there are very few studies that link manipulation of executive regulators to changes in

Lack of detailed knowledge limits the potential for intervention The ability to modulate carbon fate in a predictable way would have enormous implications for prevention and treatment of cancer, Type 2 Diabetes, and other diseases characterized by metabolic dysregulation. However, we have very limited understanding of how executive regulators like AMPK and PKA actually influence metabolism. With some exceptions,<sup>9</sup> attempts to control the respirofermentative balance in yeast by changing the concentrations of one or two enzymes at a time have met with little success. For example, when 8 enzymes for glycolysis and ethanol formation were overexpressed separately and in pairs with little effect on ethanol formation.<sup>10</sup> There have been only a few attempts to influence metabolic outcomes in yeast by modifying transcriptional regulation, but the success rate of these few efforts has been much higher than that of the direct approach.<sup>11-13</sup> By analogy, if you want to influence the output of a factory, you would be much more likely to succeed by influencing managers than by manipulating individual line workers.

Our ability to intervene in the AMPK and PKA pathways is severely limited by the current state of knowledge of the logic governing AMPK and PKA integration. We know almost nothing about why particular TFs are regulated by AMPK, PKA, or both. Similarly, we do not know why particular enzymes within a metabolic pathway regulated by specific TFs while other enzymes within the same pathway are regulated by other TFs. In order to design effective interventions, we must understand this organization both qualitatively and quantitatively. Without a quantitative model, we cannot predict the net effects of interventions in this complex network, which contains numerous feedback and feed forward loops, on gene expression and metabolism. Successful completion of this project will yield such a predictive model. It will also provide a much clearer picture of how strategic decisions about carbon fate are implemented. We will have an integrated model of how effector TFs, the foremen of the metabolic factory, influence carbon fate. Characterizing the link between executive regulators and carbon fate is an essential first step toward controlling metabolic output to improve human health.

TF activity, changes in gene expression, and changes in metabolic flux. **Our study is innovative because it will link two specific regulatory pathways to a specific metabolic response: the shunting of carbon toward biomass, fermentation, or respiration.** Our goal is to understand, on a quantitative level, the messages sent by two execu-

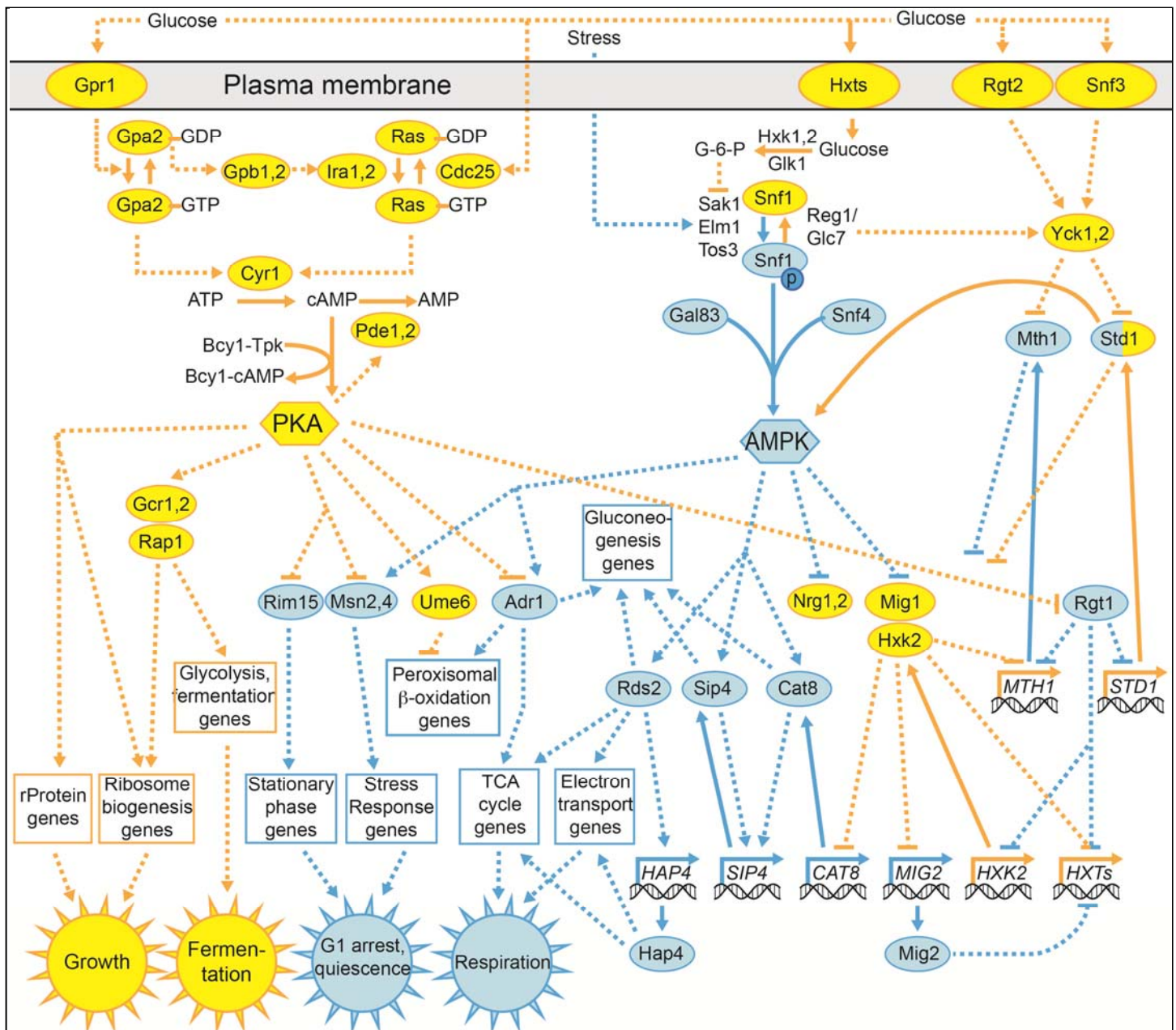


**Fig. 1** Partial sketch of the overlapping PKA and AMPK pathways. Gold: more active in higher glucose concentrations. Blue: more active in low glucose or no glucose. *MTH1* and several *HXT* (hexose transporter) genes are repressed in both high and low glucose but are expressed at intermediate concentrations. Dotted lines with arrow heads: activation; dotted lines with flat heads: repression; solid lines: covalent or non-covalent transformation.

tive regulators to the end effectors of transcriptional regulation and how responsibility for carbon fate is divided among end effectors.

Our approach is also innovative. While we make use of genome-wide RNA profiling, our focused approach is genetic and metabolic rather than genomic or metabolomic. It has the following innovative combination of features:

1. Manipulation of AMPK and PKA by both genetic and environmental means. We will express key genes in these signaling pathways at multiple levels under the control of doxycycline repressible promoters. Each pathway will be manipulated in wild type cells and in a mutant where signaling in

the other pathway is held constant. Cells will be grown in both excess glucose and limiting glucose.

2. Quantification of the effective activity of AMPK and PKA and their effects on metabolism in each strain and condition. We will quantify the activity of these executive regulators by analyzing the expression pattern of their downstream targets. We will also quantify carbon fate in wild type and in mutants with perturbed PKA and AMPK activity levels.
3. Quantification of the activity of end effector TFs and their effects on metabolism in each strain and condition. We will delete end effector TFs

and quantify the effects of these deletions on gene expression and carbon fate.

4. **Predictive modeling.** Using the treasure trove of data generated for Aims 1 and 2, we will construct an integrated, quantitative model of the functioning of the AMPK and PKA pathways. Currently, there is no model that can predict carbon fate as a function of activity in signaling pathways.

These data and models will provide the first integrated understanding of how signals from AMPK and PKA are integrated through their effects on TF activity, gene expression, and carbon fate.

## INVESTIGATORS

An outstanding team of investigators has been assembled to pursue these important aims. Brent is a recognized expert in mathematical and computational modeling who has developed significant expertise experimental yeast biology. Johnston is an internationally acclaimed yeast geneticist who first elucidated the roles of the glucose sensors *Rgt2* and *Snf3* and the downstream network, including *Rgt1*, *Mth1*, and *Std1* (Fig. 1, right),<sup>17-21</sup> and played a leading role in the yeast deletion strain project.<sup>22,23</sup> The proposed work is a natural extension of a productive collaboration between Brent and Johnston,<sup>24</sup> who hold joint video conferences with all project personnel every other week. Doering is an internationally recognized biochemist with whom Brent has a history of collaboration.<sup>25,26</sup> They are currently mapping the network that regulates the size of the polysaccharide capsule of the fungal pathogen *Cryptococcus neoformans* (which includes PKA). They co-supervise a Ph.D. student doing outstanding work in both basic modeling algorithms and *Cryptococcus* biology. They hold bi-weekly meetings with all project personnel.

## APPROACH

### Background

A partial sketch of the AMPK and PKA signaling pathways and their functional effects is shown in Fig. 1, which we made by carefully analyzing and integrating recent literature and publicly available data sets. Fig. 2 shows the regulation of some key pathways in energy metabolism from a metabolo-centric perspective, linking individual enzymes to their regulators from Fig. 1. Figure 2 is derived from literature, publicly available data sets, and our own, unpublished RNA-seq data from cultures before and after diauxic shift.

Yeast cells lacking *Snf1* (the yeast protein that serves as the catalytic component of the AMPK complex) have been studied and many genes that are transcriptionally affected by the *Snf1* deletion have

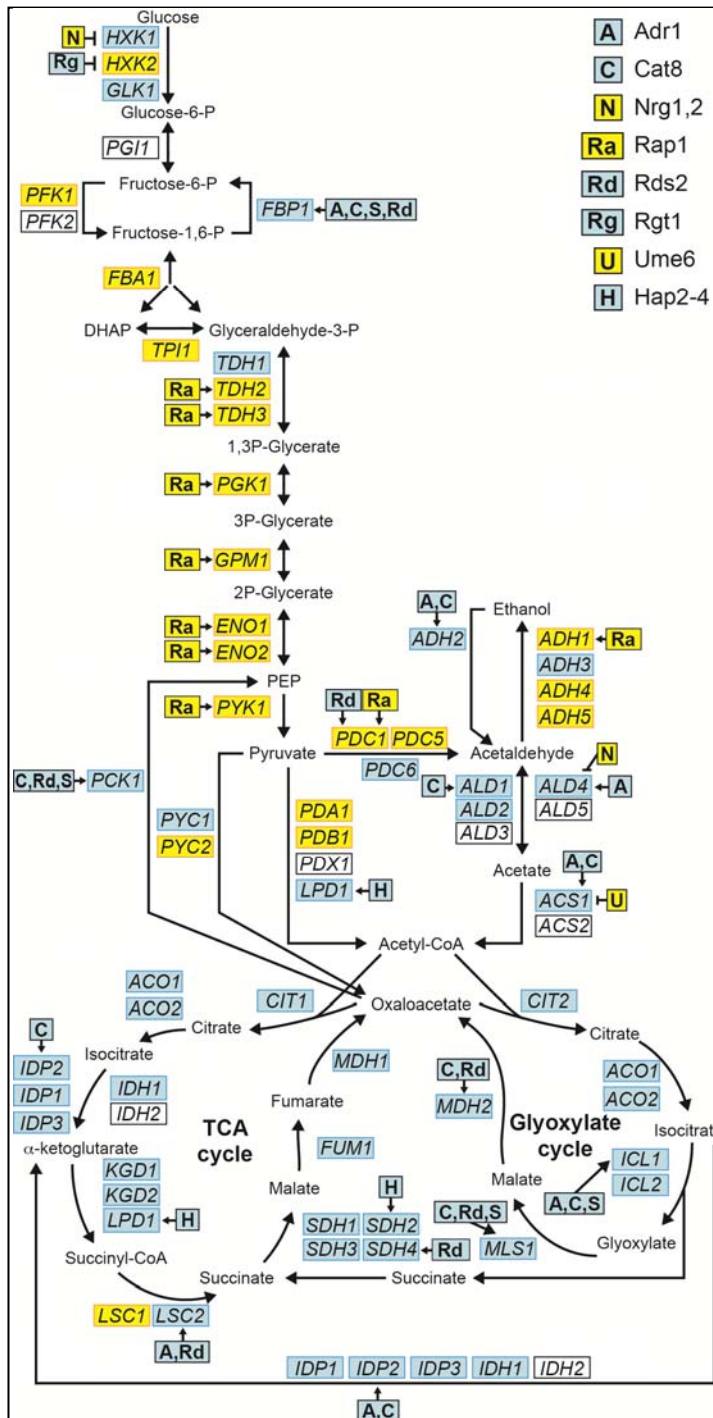


**Fig. 2** Metabolic pathways annotated with enzymes that catalyze each reaction and transcription factors from Fig. 1 that regulating each enzyme. Gold: more highly expressed (enzymes) or more total activity (transcription factors) in excess glucose; blue: more highly expressed or more total activity in low glucose or alternative carbon sources. Compartmentalizing and trafficking proteins are not shown.

been identified.<sup>1,27</sup> Specific TFs that serve as end effectors of the AMPK pathway are also known (Fig 1).<sup>28-32</sup> The PKA heterotetramer is composed of two catalytic subunits (encoded by *TPK1*, *TPK2*, or *TPK3* in yeast) and two regulatory subunits (encoded by *BCY1* in yeast). Provision of excess glucose leads to a rapid increase in intracellular cyclic AMP (cAMP)



which binds to Bcy1, the inhibitory subunit of PKA, causing it to dissociate from the complex (Fig. 1). Any one of the *TPK* genes is sufficient for growth, but the triple deletion is lethal. Cells in which PKA has been constitutively activated by deletion of *BCY1* or by the activated *RAS2*<sup>19</sup> allele are sensitive to nutritional deprivation and fail to arrest in G1 in response to starvation,<sup>33</sup> presumably because they fail to inactivate PKA. PKA phosphorylates and modulates the activity levels of a number of known the yeast TFs some of which are shown in Fig. 1.

Several recent studies have begun to shed light on various parts of the regulatory apparatus depicted in Fig. 1 and their influence on the metabolic pathways depicted in Fig. 2. Darin-Lapides and colleagues grew yeast cells in steady-state, continuous-flow chemostat cultures on growth-limiting quantities of glucose, maltose, ethanol, or acetate.<sup>16</sup> For each carbon source, they measured gene expression, oxygen consumption, CO<sub>2</sub> production, residual nutrient concentration, and the metabolic products ethanol and acetate. In total, 95-97% of input carbon was recovered. With the exception of the acetate culture, essentially all of the input oxygen was recovered as CO<sub>2</sub>, indicating full aerobic respiration. Flux through individual metabolic reactions was estimated using a flux balancing model.<sup>34-36</sup> However, the AMPK and PKA pathways do not respond to carbon source per se but rather to energy balance.<sup>37</sup> Excess energy was absent in all these cultures, where carbon sources at very low extracellular concentration were growth limiting. Under these conditions the AMPK complex is expected to be active and the PKA complex inactive (Fig. 1). Perhaps because the activity levels of these complexes did not change significantly from one carbon source to another, this study identified a total of only 180 genes that reliably changed expression by two-fold or more between any of the carbon sources, while at least 1800 genes change between conditions of excess glucose and ethanol.<sup>14</sup>

In another study linking transcriptional regulation to metabolism, Usaite and colleagues compared wild-type cells to strains lacking *SNF1* (the yeast gene encoding the catalytic subunit of AMPK), *SNF4* (the yeast gene encoding the regulatory subunit), or both, after growth in carbon-limited chemostat cultures<sup>27</sup> The numbers of differentially expressed transcripts in these strains, compared to wild type, were 1651, 1810, and 2395, respectively. Forty-four intracellular metabolites were quantified by gas chromatography coupled to mass spectrometry, and a flux balance model of all *S. cerevisiae* metabolism was used to estimate fluxes through the network.<sup>35</sup> A number of

genomic and metabolomic network analyses were carried out, including DOGMA analysis, Reporter Metabolite analysis,<sup>38</sup> and Reporter Effector analysis.<sup>39</sup> Each of these analyses identified different, but related, networks downstream of Snf1.<sup>4</sup> This genomic-metabolomic study was looking for any effects of AMPK perturbation under energy limiting conditions, rather than focusing on carbon fate. It did not involve studies in excess glucose or manipulation of PKA.

Fendt et al.<sup>40</sup> screened 119 TF deletion mutants for effects on metabolic fluxes in batch cultures growing in minimal medium with 1% glucose, 1% galactose, 1% glucose plus high osmolarity, 1% glucose plus low pH, and 1% glucose with urea as nitrogen source. They identified 23 TFs that affect respiration by reducing flux through the TCA cycle in an average of two conditions each. They further investigated the four TFs that increased respiration in all four of the excess glucose conditions (*Bas1*, *Gcn4*, *Gcr2*, and *Pho2*) with protein mass spectrometry, confirming increases in certain TCA cycle enzymes. They also carried out transcriptional profiling on these four mutants in order to identify TFs downstream of them. TFs that strongly reduce respiration during growth on galactose were also identified: *Hap2-5* (which form a complex), *RTG1,3* (which are activated by impaired mitochondrial function), *Leu3*, and *Mac1*. This study also identified two enzymes that were consistently upregulated when respiration was increased (*Cit1* and *Mdh1*) and two that were upregulated in strains showing the greatest increase in respiration (*Idh1* and *Idh2*). This study did not involve direct manipulation of the PKA or AMPK pathways nor did it include any conditions in which hexose concentration was growth limiting.

Slattery and colleagues investigated the effects inactivating combinations of TOR, PKA, and glucose import (which lies upstream of AMPK) on gene expression when completely starved, quiescent cells are resuspended in excess glucose.<sup>1</sup> They found that simultaneous blockage of TOR, PKA, and glucose import essentially eliminated the transcriptional response. Overall, PKA had the greatest impact on the transcriptional response, glucose transport (including the AMPK response) had the second largest impact, and TOR alone had the least impact. However, elimination of TOR signaling in cells with inactivated PKA significantly amplified the effects of PKA inactivation. This study shed light on the relative contributions of the three pathways to the transcriptional response, but it did not measure the contributions of effector TFs or the impact of pathways or end effectors on metabolic outcome.

Despite a recent surge of interest in major energy response pathways and their downstream impacts, no study to date has linked genetic and nutritive manipulation of these pathways to the implementation of their signals by effector TFs and the impact of each pathway and effector on metabolic outcome. Our study will provide a far more complete and integrated picture of how PKA and AMPK interact with each other and their effector TFs to remodel central carbon metabolism. Furthermore, we will produce the first integrated, quantitative model of gene regulation by AMPK and PKA.

### Preliminary and related studies

**Regulation of glucose transporter genes** We recently produced a predictive, quantitative model of the regulation of hexose transporter genes *HXT1-4* by the pathways involving *RGT1* and *SNF1*/AMPK (Fig. 1, right). Our model consists of 24 ordinary differential equations with 81 parameters. We were able to obtain 33 of these from existing high-throughput data: the rate constants for translation, mRNA degradation, and protein degradation for each gene product. We obtained 8 rate constants for glucose transport from literature and measured 30 transcriptional regulation parameters ourselves. The remaining parameters were optimized to fit a subset of our data.

Using this approach, we were able to predict the steady state mRNA levels of *HXT1-4* in 2% glucose and 2% galactose for wild-type cells and for a variety of mutants (Fig. 3). We were also able to predict the dynamics of *HXT1-4* expression after addition of 0.1% glucose to a culture grown on galactose (Fig. 4 shows one example). This approach required simultaneous deletion or inactivation of all transcription factors acting on the *HXT* genes, which is not practical for the much larger network we will investigate in this project. However, the quantitative and qualitative knowledge we gained in this study, as well as the experience in working with the response of *snf1Δ*, *mig1Δ*, *mig2Δ*, and *rgt1Δ* mutants, has prepared us for the current project.

**Global effect of *SNF1* deletion on gene expression** In an as-yet unpublished investigation, we deleted *SNF1* from a Xylose-fermenting strain<sup>41</sup> derived from

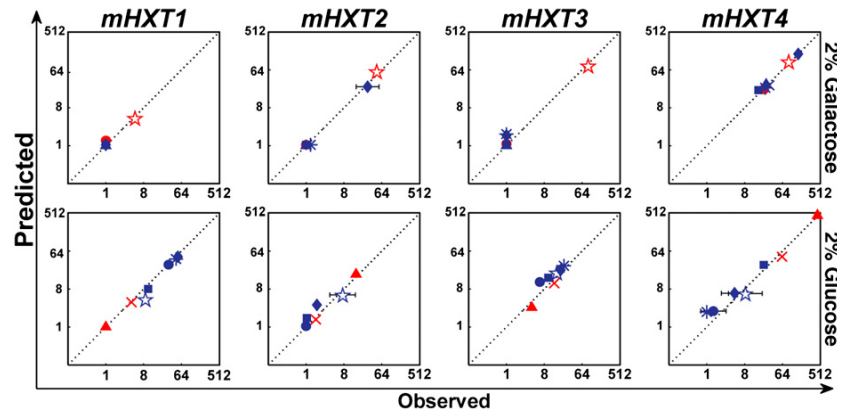


**Fig. 3** Observed and predicted steady-state levels of *HXT1-4* mRNAs in cells grown in 2% galactose (Upper) or 2% glucose (Lower). Units are molecules per 81 ACT1 molecules (an estimate of the number of ACT1 molecules per yeast cell). Each data point represents a TF deletion strain. Circles, WT; stars, *rgt1Δ*; diamonds, *mth1Δ*; asterisks, *std1Δ*; crosses, *mig1Δ*; squares, *mig2Δ*; triangles, *mig1Δ mig2Δ*. Error bars indicating one SEM are shown for the measurements with the largest errors (the others would not be clearly visible). Data points that were used to calculate  $V_i$  and  $\Theta_{ij}$  are in red and independent tests of the model are in blue. Each point is predicted by a model whose optimized parameters are fit to the other points.

CEN.PK2-1D, chosen to facilitate comparison with a recent microarray study.<sup>42</sup> The deletion strain (*snf1Δ*) and the parental strain (WT) were grown in synthetic complete media with 2% glucose and 5% xylose. Samples taken at 4 hours (when about half of the glucose was consumed) and 24 hours (10 hr after all glucose was consumed).

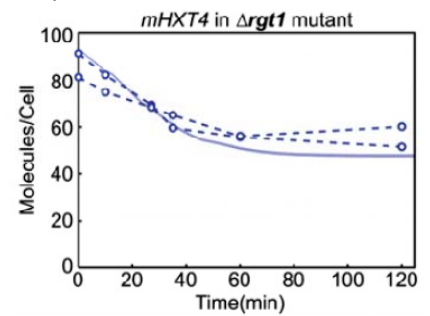


**Fig. 4** Solid line: prediction of our model for the time course of *HXT4* mRNA in *mig2Δ* cells after addition of 0.1% glucose to a galactose culture. Circles: quantitative PCR data. about half of the glucose was consumed) and 24 hours (10 hr after all glucose was consumed).

For expression profiling by RNA-seq, samples were bar coded and sequenced six per lane (we now do 12 per lane on the Hi-Seq machine). The reads were mapped back to the yeast genome (using TopHat<sup>43</sup>) and converted to expression levels (using Cufflinks<sup>44</sup>), which were normalized to the 75<sup>th</sup> percentile within each sample<sup>45</sup>. *SNF1* mRNA was detected at approximately the same level in all WT samples but was not detected in any of the *snf1Δ* samples, as expected.

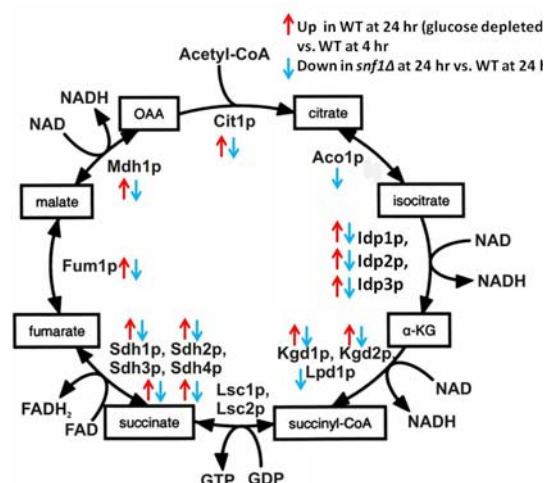


**Fig. 5** Deletion of *SNF1* moves expression of TCA cycle genes at 24 hr, when glucose has been exhausted, toward their expression levels in WT cells at 4 hr, when glucose remains. Red arrows: genes that are significantly up regulated subsequent to glucose exhaustion in wild type cells; blue arrows: genes that are significantly down regulated at 24 hr as result of *SNF1* deletion.

Overall, *SNF1* deletion moved the expression profile after glucose exhaustion closer to the WT profile before glucose exhaustion: The Euclidean distance between expression states of WT 4 hr and WT 24 hr was 469, whereas the distance between WT 4

hr and *snf1Δ* 24 hr was only 430. However, *snf1Δ* 24 hr remained much closer to WT 24 hr (distance 203) than to WT 4 hr. 2,680 of 6,490 total genes were differentially expressed at 24 hr as a result of the *SNF1* deletion according to the analysis program ELNN<sup>46</sup> (2,702 according to LIMMA<sup>47</sup>). Genes encoding enzymes that catalyze the irreversible steps of glycolysis were significantly up regulated in the *snf1* mutant at 24 hr, whereas genes encoding enzymes that catalyze the corresponding steps of gluconeogenesis were down regulated or unchanged.

Almost all genes encoding enzymes of the TCA cycle were significantly down regulated by the *SNF1* deletion, moving their expression at 24 hr toward their levels in WT at 4 hr (Fig. 5).

**Aim 1** Elucidate the influence of master regulators AMPK and PKA on gene expression and carbon fate.

#### Aim 1: Rationale

Aim 1 will provide answers the questions

1. How sensitive are gene regulation and carbon fate to changes in the activity levels of PKA and AMPK in excess or growth limiting glucose?
2. What is the logic by which PKA and AMPK activity interact to influence carbon fate? Quantitatively, how does the activity level of PKA or AMPK affect sensitivity to the activity level of the other?
3. Is it possible to decouple the balance of respiration and fermentation from growth rate, at least temporarily, by independently manipulating the activity levels of PKA and AMPK?

#### Aim 1: Overview of approach

Both positive and negative regulators of PKA and AMPK will be put under control of a doxycycline-repressible tet promoter ( $P_{tet}$ ) in order to control the activity levels of these pathways independently of glucose concentration. We will grow these mutants (and wild type controls) with varying concentrations

of doxycycline in oxygenated chemostats, carefully monitoring consumption of glucose and oxygen and all significant carbon and oxygen outputs. From these measurements we will calculate quantitative indices of growth, fermentation, and respiration. We will also carry out transcriptional profiling by RNA-seq. Analyses of transcript levels will give a quantitative index of pathway activity that is independent of doxycycline concentration.

#### Aim 1 Task 1: Construction of mutant strains

In this study, we will use the strains described in Table 1 (left). Table 1 also indicates the predicted activity levels of PKA and AMPK in cultures of each strain growing in limiting or excess glucose and in the presence or absences of doxycycline. In Strain 2 (*bcy1Δ:P<sub>tet</sub>-BCY1*), *Bcy1*, the negative regulatory subunit of PKA, is expressed under the control of a doxycycline repressible promoter, so the addition of dox activates PKA in limiting glucose by freeing it

No.	Genotype	Limiting glucose				Excess glucose			
		PKA		AMPK		PKA		AMPK	
		-dox	+dox	-dox	+dox	-dox	+dox	-dox	+dox
1	Wild type (BY4741/B4742)	L	L	H	H	H	H	L	L
2	<i>bcy1Δ:P<sub>tet</sub>-BCY1</i>	L-	H+	H	H	H-	H+	L	L
3	<i>tpk1Δ:P<sub>tet</sub>-TPK1 tpk2Δ tpk3Δ</i>	L?	L-	H	H	H?	L-	L	L
4	<i>reg1Δ:P<sub>tet</sub>-Reg1</i>	L	L	H-	H+	H	H	L-	H+
5	<i>snf1Δ:P<sub>tet</sub>-SNF1</i>	L	L	H+	L-	H	H	L+	L-
6	<i>tpk1Δ:P<sub>tet</sub>-TPK1 tpk2Δ tpk3Δ reg1Δ:P<sub>tet</sub>-REG1</i>					H?	L-	L-	H+
7	<i>bcy1Δ:P<sub>tet</sub>-BCY1 snf1Δ:P<sub>tet</sub>-SNF1</i>	L-	H+	H+	L-				

**Table 1** Strains and predicted pathway activity levels in each experimental condition. H: high. L: Low.

from Bcy1 inhibition. In Strain 3 (*tpk1Δ:P<sub>tet</sub>-TPK1 tpk2Δ tpk3Δ*) the most active catalytic subunit of PKA is doxycycline repressible and the other two are deleted, so addition of doxycycline represses PKA activity in high glucose. In strain 4 (*reg1Δ:P<sub>tet</sub>-REG1*) *Reg1*, a negative regulator of AMPK activity, is doxycycline repressible, so the addition of doxycycline activates AMPK in excess glucose. In Strain 5 (*snf1Δ:P<sub>tet</sub>-SNF1*) *Snf1*, the catalytic subunit of AMPK, is doxycycline repressible, so addition of dox represses AMPK activity in limiting glucose. Strain 6 combines the mutations of Strains 3 and 4, allowing the activity levels of both PKA and AMPK to be switched simultaneously in excess glucose. Strain 7 combines the mutations of 2 and 5, allowing the activity levels of both PKA and AMPK to be switched in limiting glucose. Addition of doxycycline would have a relatively small effect on Strain 6 in limiting glucose and on Strain 7 in excess glucose, so these experiments will not be done.

#### Aim 1 Task 2: Growth of chemostat cultures and measurement of metabolic inputs and outputs

The strains in Table 1 will be grown in chemostats with excess or limiting glucose. For each strain and glucose condition, we will grow cultures at four levels of doxycycline that span the range from over expression at a level comparable to the actin gene *ACT1* (~90 mRNA molecules per cell in the absence of doxycycline) to 200-1000 fold lower (at 1.0µg/ml), based on the Brent Lab's experience with this plasmid. Adding two intermediate levels (0.001µg/ml, 0.05 µg/ml) produces a set of four expression levels in steps of 6-10 fold (data not shown). (Doxycycline has no discernable effect on the expression of native genes in *S. cerevisiae*,<sup>48</sup> however we will grow WT in all dox conditions as a control to be certain.) The total number of strain-by-glucose-by-dox conditions will be 48, each of which will be run three times using independent transformants.

Initially, all cultures will be brought to steady-state in glucose limiting continuous flow mode at 30 °C in the Brent Lab's two BioFlo 110 2-liter chemostats (New Brunswick Scientific) essentially as described.<sup>16,49</sup> Cultures will be fed defined minimal medium with growth-limiting glucose (5g/L) and all other growth requirements in excess, with a dilution rate of 0.10/hr. The pH will be measured on-line and kept constant at 5.0 by the automatic addition of 2 M KOH. Dissolved oxygen tension will be measured online. Cultures will be aerated at 0.5 L/min while stirring at 800 rpm. The off-gas will be automatically analyzed using the EX-2000 O<sub>2</sub>/CO<sub>2</sub> off-gas analyzer

(New Brunswick) located in the Brent Lab. The inflow medium will then be changed to contain doxycycline and/or glucose, according to the experimental condition, for 120 minutes, to specified final concentrations of dox and final concentrations of glucose of about 10 g/L. This interval is sufficient for completion of most of the primary and secondary transcriptional responses to glucose increase and for metabolic adjustment, without being so long that population growth causes the increased glucose feed to become limiting again.<sup>50</sup> While we expect most transcripts to have approached a new steady state, residual changes in the levels of a few transcripts will not significantly affect our results. Between 120 and 130 minutes after medium change, we will analyze off-gas, harvest medium for metabolite analysis, and harvest cells for RNA preparation. For low glucose cultures we will follow the same procedure without increasing the glucose concentration.

We will analyze metabolites in media samples by using the Waters HPLC with auto-sampler and in-line refractometer (Waters 2414) located in the Doering Lab (see support letter). Samples will be run through an ion-ordered partition chromatography column (Aminex HPX-87H, Bio-Rad) according to the manufacturer's protocols. Glucose, ethanol, acetic acid, lactic acid, and glycerol peaks will be detected by refractive index and identified and quantified by comparison to retention times of authentic standards. Biomass will be assayed by dry weight as described.<sup>41</sup> Residual glucose is expected to be below the detection limit for glucose limited cultures and to be on the order of 1% for excess glucose cultures. Measurement of oxygen and carbon dioxide in the off-gas, together with dry weight, residual glucose, and ethanol is sufficient to calculate the relative rates of aerobic respiration, fermentation, and growth, and to recover ~97% of input carbon. These measurements are also sufficient for modeling flux through the reactions shown in Fig. 2.<sup>16</sup> Measurements of other metabolites will provide confirmation and additional detail and may allow recovery of a small amount of additional input carbon.

#### Aim 1 Task 3: Transcriptional profiling by RNA-seq

For each of the 144 total cultures described above, we will extract RNA from cells harvested 120-130 min after medium shift. After poly-A<sup>+</sup> purification and cDNA synthesis, sequencing libraries for the Illumina Hi-Seq will be prepared (see Preliminary Studies). Samples will be prepared 12 at a time, bar-coded, and multiplexed 12-fold so that only 12 sequencing lanes will be required. Resulting sequence will be



converted to expression levels as in Preliminary Data. These methods are routine in the Brent Lab.

#### Aim 1 Task 4: Analysis of PKA, AMPK activation

We will control the activation of the PKA and AMPK pathways using glucose and doxycycline as described in Task 1. We can infer the effects of these manipulations on the activation levels of PKA and AMPK by statistical analysis of their indirect effects on transcript levels.<sup>39</sup> We will take two complementary approaches to this problem. First, we will search our RNA-seq data for a set of genes with a highly significant change in expression due to doxycycline-based manipulations of one and only one pathway and with relatively low variance within condition for all manipulations. Using RNA-seq data from all conditions, we will determine a minimum and maximum expression level for each of these genes and normalize their expression measurements, converting them to percentages of the total range for that gene. (As an alternative normalization we will also try standard deviations off the mean, which worked well for Oliveira et al.<sup>39</sup>) For each executive regulator in each condition, we will average the normalized expression of each target gene affected uniquely by it and use the average as an index of the activity of the executive regulator. We expect we will be able to identify genes that are affected uniquely or primarily by one of the executive regulators because there are effectors downstream of both PKA and AMPK that are not thought to be downstream of the other (Fig. 1). However, since many target genes that are regulated by these effectors are also regulated by effectors of the other pathway, the number of genes that are uniquely affected by each executive regulator could be small.

As a complementary activity index for each executive regulator, we will use the normalized expression levels of all genes weighted according to how strongly they are affected by doxycycline-based manipulations of the regulator. The weighting for, e.g., PKA, will be determined by principle components analysis of expression levels of all genes in all samples representing doxycycline-based manipulations of PKA. In each case, the first principle component will represent the effects of PKA manipulations. The weighted expression levels of all genes will be used as an index of PKA activity (and similarly for AMPK).

To evaluate the two indices, we will look at their correlation with the respiration/fermentation, respiration/biomass, and fermentation/biomass ratios (calculated as described below). We will also look at their correlation with each other, and their variance among replicates of the same condition. We will prefer the

index that correlates better with metabolic activity and has the least ratio of within-condition to between-condition variance.

We will validate our estimates of AMPK and PKA activity by well-established methods: Active Snf1 will be detected by immunoblotting using a commercially available monoclonal antibody specific for Snf1 phosphorylated on T210 in the activation loop, normalizing to the total level of Snf1 (determined by immunoblotting with an antibody specific to Snf1<sup>51</sup>); levels of active PKA will be determined by detecting the amount of PKA bound to its Bcy1 regulatory subunit by fluorescence resonance energy transfer.<sup>52</sup>

#### Aim 1 Task 5: Analysis of carbon and oxygen fate

We will measure the rate of aerobic respiration versus anaerobic fermentation by using both an oxygen-based and a carbon based method. The oxygen-based method is based on the relative specific rates of oxygen consumption and CO<sub>2</sub> production. If approximately one molecule of dissolved O<sub>2</sub> were consumed for every two molecules of CO<sub>2</sub> produced (the other oxygen comes from glucose) then metabolism would be purely by aerobic respiration; if no oxygen were consumed, metabolism would be purely fermentative. The second method, which should closely corroborate the oxygen method, is to compare the fraction of carbon released as CO<sub>2</sub> to the fraction released as ethanol. If one molecule of ethanol were produced for each CO<sub>2</sub> then metabolism would be purely fermentative; if no ethanol or minor fermentation products were produced then metabolism would be purely aerobic. Because these are specific rates they are already normalized to the total dry weight at the time of measurement. We also compare the specific rates of CO<sub>2</sub> and ethanol production to the growth rate – the third major carbon fate.

#### Aim1: Anticipated results

At the conclusion of this Aim, we expect to have a quantitative understanding of the interplay between PKA and AMPK activity in determining carbon fate. We will determine the sensitivity of respiration, fermentation, and growth, to the activity of each of these pathways, as a function of the activity of the other and the availability of excess glucose. This will shed light on the degree to which fermentation rate and growth rate can be decoupled through manipulation of these executive regulators, and will provide a starting point for Aim 2, in which we will carry out the similar analyses at the level of end effector TFs.

#### Aim1: Possible challenges and alternative methods

The Brent lab has extensive experience in the construction and use of yeast strains in which specific ORFs are driven by doxycycline-repressible promoters, so we do not anticipate any general difficulties. Haploid strains carrying deletions of *BCY1*, *REG1*, and *SNF1* are all viable in glucose, but even if they were not, we could grow our conditional mutants in the absence of doxycycline. Strains lacking *TPK2* and *TPK3* are viable as long as *TPK1* is expressed, which will be the case in our conditional deletion in the absence of doxycycline. After saturating doxycycline is added to cultures there is still a very small amount of transcription which may provide sufficient Tpk1 for growth. Even if residual transcription is not sufficient for growth, our cells only need to survive for 130 minutes after the shutdown of *TPK1* transcription by doxycycline; growth is not required. As an alternative we can transform  $P_{tet}$ -*TPK1* into the *tpk-w* mutant, which has low-level PKA activity that is unresponsive to changes in cAMP levels in the cell.<sup>53</sup> Over expression of *BCY1*, *TPK1*, *REG1*, and *SNF1* is not expected to be toxic but if problems of this kind are encountered we can add doxycycline to reduce expression and/or reduce the number of tetO binding sites in the promoter.<sup>54</sup> Another alternative is to de-

lete *CYR1*, encoding adenylate cyclase, and control PKA directly through addition of cAMP.<sup>1</sup> Finally, note that no single strain or condition is essential to the success of this aim.

Doxycycline titration provides quantitative control over the transcription of genes controlled by the tet-off system, but this control is not precise and transcription rates at low dox concentrations can vary somewhat from strain to strain and condition to condition. However, it is not crucial that we achieve four distinctive expression levels for each dox controlled ORF; three would be sufficient and even two would provide the information that is essential to the project. However, we are using four distinct dox levels because we do not know in advance which ones will drive expression in the range where carbon fate is most responsive. Similarly, the project could be successful with either the oxygen-based index of respiration (which does not require quantification of glucose and ethanol) or the carbon-based index; using both will provide additional controls and validation but both are not strictly required. Enzymatic assays for glucose and ethanol also provide an alternative to HPLC assays.

**Aim 2** Quantify the role of each effector TF in mediating the influence of PKA and AMPK on gene expression on carbon fate.

#### Aim 2 rationale

Aim 2 focuses on the end-effector TFs and the way in which they translate strategic directions from the executive regulators into operational changes in enzyme levels and metabolic fluxes. To understand operational responsibilities of each TF, we must answer these questions:

1. How sensitive are gene regulation and carbon fate to changes in the activity of end effector TFs, in both excess and limiting glucose?
2. What is the logic by which end effectors interact to influence carbon fate? Quantitatively, how does the activity level of one end effector modulate the influence of the other end effectors on gene regulation and on carbon fate?
3. Is it possible to decouple aerobic versus anaerobic metabolism from slow vs. fast growth, at least temporarily, by manipulating individual end effectors?

#### Aim 2 overview of approach

Expression of 12 end effector TFs will be either eliminated or attenuated in order to perturb their total activity independently of glucose concentration, PKA, and AMPK. We will grow these mutants in excess and limiting glucose conditions, monitoring metabolic

inputs and outputs, and calculate quantitative indices of growth, fermentation, and respiration. We will also carry out transcriptional profiling and use changes in target gene expression to calculate a quantitative index of effector activity. The results of these experiments, together with those of Aim 1, will enable us to calculate the strengths of the following interactions:

1. The action of PKA and AMPK on each end effector
2. The action of each end effector on expression of each metabolic target gene
3. The action of each end effector on respiration, fermentation, and growth

With these quantities we can begin to understand the contribution of each end effector to the overall influence of each executive regulator on metabolic outcome. This will lay the ground work for building a quantitative model that links AMPK and PKA activity levels to carbon fate.

#### Aim 2 Task 1: Construction of mutant strains

The end effector TFs we will focus on are Rap1, Ume6, Adr1, Rds2, Hap4, Sip4, Cat8, Nrg1, Nrg2, Mig1, Mig2, and Rgt1 (see Figs. 1 and 2). Rim15,

Msn2, and Msn4, which do not appear to directly regulate genes of central carbon metabolism, will not be in our core TF set at the outset, but we will add them if our data indicate that they should be included. Null mutants in all these genes are viable with the exception of *rap1*. The viable null mutants are in the yeast deletion strain library<sup>22,23</sup> and will be grown from stocks in our labs. Null mutants of each of the 12 viable strains will be crossed with Strains 2-5 from Table 1, allowing quantitative control of PKA and AMPK activity. Since *rap1* is lethal, we will use an existing conditional mutant in which *RAP1* expression can be titrated by addition of doxycycline,<sup>55</sup> but we will not cross it into the strains from Table 1 because the effect of doxycycline on pathway activity would be confounded by its effect on *RAP1* expression.

#### Aim 2 Task 2: Growth and quantitative characterization of effector-TF single mutants

Each of the 12 single-TF null mutants will be cultivated in a chemostat in both excess and limiting glucose as described in Aim 1. The  $P_{tet}$ -*RAP1* strain will

be cultivated along with doxycycline at 4 different concentrations. Over expression of *RAP1* is toxic, too, so we will use 4 dox levels to find in which  $P_{tet}$ -*RAP1* is viable (even if growth is slow after additional of dox). We will run 3 additional replicates of WT in order to improve statistical power for detecting changes. Metabolic inputs and outputs will be measured in triplicate cultures in all conditions.

#### Aim 2 Task 3: Transcriptional profiling by RNA-seq

Transcriptional profiling by RNA-seq will be carried out on all samples as described in Aim 1. With our standard 12-way multiplexing we anticipate that 7 or 8 sequencing lanes will be needed, in total.

#### Aim 2 Task 4: Analysis of effector-TF activation

The activity levels of effector TFs will be calculated as described for the executive regulators in Aim 1.

#### Aim 2 Task 5: Analysis of carbon and oxygen fate

We will measure the rates of respiration, fermentation, and growth in all cultures as described in Aim 1.

### **Aim 3 Build an initial quantitative model linking PKA and AMPK to metabolic outcomes via effector TFs.**

#### Aim 3: Rationale

Aims 1 and 2 will provide quantitative activation levels of PKA and AMPK under a variety of conditions, the activation levels of their effector TFs, the expression levels of all genes, and the rates of growth, respiration, and fermentation. Having made quantitative measurements, we will be in position to make a predictive, quantitative model. Such a model is necessary to predict the net effects of potential interventions in a complex system that exerts many counterbalancing forces on gene expression and carbon fate. This model will also provide hypotheses for future work beyond the scope of this proposal, including experiments and interventions on mammalian cells.

#### Aim 3: Overview of approach

Our approach to regulatory modeling (Task 1) will closely follow the approach we used successfully to model the regulation of hexose transporters,<sup>24</sup> except that we will focus on approximately steady state conditions. We will write a series of equilibrium equations representing most of the reactions in Fig. 1, focusing on the reactions downstream of PKA and AMPK. These equations will contain many unknown parameters, which we will estimate using the expression and activation values from Aims 1 and 2.

#### Aim 3, Task 1: regulatory modeling

Models of transcription-factor activation Each transcription factor protein is modeled as having an active and an inactive state. For each TF, the active fraction is determined by irreversible phosphorylation catalyzed by PKA and/or AMPK and in some cases

by reversible protein-protein binding (including oligomerization). Irreversible reactions are assumed to be at equilibrium with the production and degradation of the reactants. For example, the phosphorylation of Mig1 by Snf1 and its subsequent active degradation (Fig. 1) is assumed to be at equilibrium with the production and passive degradation of Mig1. Protein-protein binding reactions are assumed to be at equilibrium with dissociation. Unknown equilibrium constants must be obtained indirectly by fitting to data collected for Aims 1 and 2, as described below.

Proportionality of mRNA and protein levels As in our previous work on *HXT* genes, we assume that the concentration of each TF protein at steady state is roughly proportional to its mRNA concentration. We do not assume that the proportionality constant is known or is the same for each protein; thus, the relative levels of two different proteins cannot be determined simply by comparing their mRNA levels.<sup>56,57</sup> Given these assumptions, equilibrium constants can be used in conjunction with mRNA concentrations as follows. If  $m_i$  is the concentration of mRNA  $i$  (assumed to be proportional to the concentration of protein  $i$ ), and if  $k_i$  is the equilibrium constant between active and inactive forms of protein  $i$ , then  $m_i k_i$  is proportional to the concentration of active protein  $i$ .

Transcriptional regulation function We will use a transcriptional regulation function that is inspired by the so-called “thermodynamic model”. This general approach to modeling transcriptional regulation was pioneered by Shea and Ackers<sup>58</sup> and has had a number of recent successes.<sup>59-66</sup> In our adaptation of

this approach, the form of the function that predicts transcript levels in a given strain and condition:

$$D_i m_i^R = \alpha / \left[ 1 + \frac{\prod_{j \in R} (1 + c_{i,j} m_j^R)}{r_i \prod_{j \in R} (1 + \omega_j c_{i,j} m_j^R)} \right] \quad (1)$$

where  $D_i$  is the degradation rate constant for mRNA  $i$ ,  $m_i$  is the concentration of mRNA  $i$ ,  $R$  is the set of non-deleted regulators of gene  $i$  in the strain where the measurement was made, and  $\alpha$  is the maximum possible transcription rate for any gene. Each  $m_j^R$  on the right hand side is the mRNA concentration of a transcription factor that regulates gene  $i$  (so  $m_j^R$  is zero if TF  $j$  is deleted in the strain where the measurement was made). The parameter  $r_i$  determines the transcription rate of gene  $i$  in the absence of any TF that regulates gene  $i$  ( $R = \emptyset$ ). The parameter  $\omega_j$  describes the effect of protein  $j$  on its target genes: if  $0 \leq \omega_j < 1$  then  $j$  represses its targets; if  $1 < \omega_j$  then  $j$  activates its targets; if  $\omega_j = 1$  then  $j$  has no effect on transcription. The parameter  $c_{i,j}$  modulates the strength with which TF  $j$  represses or activates gene  $i$  in particular. (If a TF directly activates some targets and represses others it can be modeled as though it were two separate TFs.) To link Equation (1) to the signal transduction network, we multiply the concentration of each TF mRNA by the fraction of the corresponding protein that is predicted to be active (not shown in Eq. 1).

Calculation of residuals for parameter estimation A version of Equation (1), modified to reflect the equilibria between activate and inactive forms of each TF, will be written for each RNA-seq data set and for each target gene within that data set. We will exclude only target genes that show no evidence of differential expression in any of our TF deletion strains. This large set of equations will be used to calculate the residual (the difference between prediction and observation) for each measurement of each target gene in each experiment. We will estimate parameter values as described below using the supercomputing cluster the Brent Lab shares with the Center for Genome Sciences and Systems Biology.

Limits of the modeling framework and alternatives A model is not intended to be an exact replica of a real system but rather to facilitate certain kinds of predictions about it under certain conditions. Our models are intended to make predictions about average RNA levels and carbon fates in populations of cells. As a result, they do not model the stochastic behavior that can arise within individual cells. Furthermore, we do not currently plan to include explicit models of cellular compartments or localization for our regulatory model, although they will be used in metabolic flux modeling. Our hypothesis (supported by success in predicting the mRNA levels of *HXT* genes) is that our mod-

els can succeed without these details (which are important for other purposes).

Estimating distributions on parameter values Rather than computing a single most likely value for each parameter in Equation (1), we will compute a marginal probability distribution on the values of each parameter. From the probability distribution, one can extract the most likely value, the expected value, confidence intervals, and other statistics indicating how precisely each parameter has been estimated.

Distributions on parameters will be estimated using a Bayesian probability model in combination with Gibbs Sampling. We define the likelihood of a given set of parameters by a normal distribution with mean zero on the sum of squared residuals. The more closely the predictions derived from a set of parameters match the data, the greater the likelihood of those parameters. Following Bayes' rule, the likelihood will be multiplied by the prior probability of the parameter values. For the parameters governing the effect of TF  $j$  on its targets,  $\omega_j$  and  $c_{1,j} \dots c_{n,j}$ , we will use a prior in which the most likely value is computed by comparing expression levels in WT to those a single-deletion strain lacking TF  $j$ . This is a quantitative analog to differential expression analysis, in which each perturbation is compared to the WT control independently.<sup>67</sup>

### Aim 3, Task 2: metabolic modeling

Our second task is to model the impact of gene regulation on metabolic pathways, including those shown in Fig. 2. We will use two complementary approaches. The more ambitious, mechanistic approach is to model the impact of gene regulation on enzyme levels and the impact of enzyme levels on metabolic fluxes. The complementary, lower risk approach is to model the impact of TF activity on metabolic outcome directly using statistical machine learning, without an intervening model of enzyme levels and fluxes through individual reactions.

Flux-based modeling Flux balance analysis (also called constraint-based metabolic analysis) is an approach to metabolic modeling that can be used to estimate the flux through each reaction in a metabolic network from the measured inputs and output of the network.<sup>16,34-36,40,68-70</sup> It relies on the stoichiometries of the reactions and on constraints such as the maximum possible flux through each reaction. Within the given constraints, the analysis algorithm finds the set of fluxes that maximizes some objective function, such as the match between predicted and observed metabolic outputs. We will begin by estimating fluxes through each reaction in each strain and condition using standard flux analysis without any constraints based on gene expression. For each enzyme we will then compute the maximum of the estimated fluxes



per RNA molecule over all our measurements from Aims 1 and 2. For each experimental condition, enzymes that are at their maximum measured flux-per-mRNA will be hypothesized as possibly limiting flux through respiration, fermentation, and biomass production. This is a more formal and automated version of the analysis that Fendt et al. carried out by hand.<sup>40</sup> It will be interesting to see whether our data support their hypotheses that levels of Cit1 and Mdh1 limit flux through the TCA cycle when flux is low and that Idh1 and Idh2 limit it at higher levels.

**A unified regulatory and metabolic model** By adding the maximum observed fluxes per mRNA molecule as constraints to the metabolic model we can link our gene regulation model to metabolic output. This would allow us to predict how changes in PKA and AMPK activity, or changes in effector TF activity, would change metabolic fluxes and hence metabolic outputs. For example, suppose we delete some combination of TFs (thereby setting their activity to zero) in some condition where we know the activity levels of PKA and AMPK, so our regulatory model can predict the activity levels of the other effector TFs. From these activity levels the regulatory model can calculate the mRNA levels for each enzyme. These enzyme expression levels can be converted to maximum fluxes through the corresponding reactions by using the observed maximum flux per mRNA, calculated as described in the previous paragraph. Finally, the mRNA-based maximum flux constraints, combined with standard stoichiometries, can be used to predict maximum respiration, fermentation, and growth rates.

**Testing the unified model** We will test the unified model at both the enzymatic and regulatory levels. At the enzymatic level, we will choose a set of up to eight enzymes comprising two that are predicted to limit fermentation in limiting glucose, two that are predicted to limit fermentation in excess glucose, and similarly for respiration. We will then make mutants in which the expression of the genes encoding these enzymes is controlled by doxycycline. We will grow cultures of these eight strains at four dox concentrations each in limiting and excess glucose. We will measure metabolic inputs and outputs and RNA expression as described in Aim 1. By analyzing these experiments, we will learn whether the mRNA level of each enzyme controls fluxes in one condition but not in the other, as predicted. We will also test the model

## **FINAL NOTE**

We are excited about the enormous potential of linking gene regulation to carbon fate through integrated experimental designs and computational models. This is an approach whose time has come. The out-

standing team we have assembled for this effort, together with our previous results and history of productive collaboration, make the probability of success high.

**High risk, high impact** The ability to predict metabolic outcome as a function of TF activity would be a high impact result that would move the field forward significantly. Even if the accuracy of our predictions is imperfect, a demonstration that this approach can work, and can be improved with further development, would be a significant step forward. This high potential reward comes with high risk. It is known that the activity of many enzymes (especially in upper glycolysis) is regulated post-transcriptionally, either by metabolites or by active degradation of mRNA or protein. This will undoubtedly impact the accuracy of our predictions in some cases, but the extent of the impact will only become clear in the course of this work. Daran-Lapides et al.<sup>16</sup> observed that, in a range of growth limiting carbon sources, enzyme levels correlated well with fluxes through gluconeogenesis and glyoxylate cycle but not with fluxes through glycolysis or TCA cycle. The lack of correlation with TCA cycle expression is likely because all their growth conditions were carbon-limited, as we and others have seen that changes in glucose availability leading to changes in the respiration-fermentation ratio are accompanied by uniform and highly significant changes in the expression of TCA enzymes (Fig. 5 and ref.<sup>40</sup>).

**Statistical modeling** As an alternative to the high-risk, high impact approach based on flux modeling, we will carry out a more abstract statistical analysis. This approach models the impact of TF activity on metabolic outcome directly, bypassing individual reactions and their enzymes. We will carry out this statistical regression analysis using methods we have developed for predicting gene expression levels (in review; see<sup>71,72</sup> for similar methods). In brief, the approach is simply to estimate the impact of the activity of each TF on fermentation, respiration, and growth, by correlating TF activity with those quantitative phenotypes across the many experimental conditions of Aims 1 and 2. Like the flux-based approach, this approach will allow us to make predictions about the effects of manipulating TF activity levels on metabolic outcomes.

standing team we have assembled for this effort, together with our previous results and history of productive collaboration, make the probability of success high.

## REFERENCES CITED

1. Slattery, M.G., Liko, D. & Heideman, W. Protein kinase A, TOR, and glucose transport control the response to nutrient repletion in *Saccharomyces cerevisiae*. *Eukaryot Cell* **7**, 358-67 (2008).
2. Hardie, D.G. AMPK and SNF1: Snuffing Out Stress. *Cell Metab* **6**, 339-40 (2007).
3. Zaman, S., Lippman, S.I., Zhao, X. & Broach, J.R. How *Saccharomyces* responds to nutrients. *Annu Rev Genet* **42**, 27-81 (2008).
4. Hong, S.-P., Leiper, F.C., Woods, A., Carling, D. & Carlson, M. Activation of yeast Snf1 and mammalian AMP-activated protein kinase by upstream kinases. *Proc Natl Acad Sci U S A* **100**, 8839-8843 (2003).
5. Wittig, R. & Coy, J.F. The role of glucose metabolism and glucose-associated signalling in cancer. *Perspect Medicin Chem* **1**, 64-82 (2008).
6. Zhou, G. et al. Role of AMP-activated protein kinase in mechanism of metformin action. *J Clin Invest* **108**, 1167-74 (2001).
7. Fryer, L.G., Parbu-Patel, A. & Carling, D. The Anti-diabetic drugs rosiglitazone and metformin stimulate AMP-activated protein kinase through distinct signaling pathways. *J Biol Chem* **277**, 25226-32 (2002).
8. Baur, J.A. et al. Resveratrol improves health and survival of mice on a high-calorie diet. *Nature* **444**, 337-42 (2006).
9. Peter Smits, H. et al. Simultaneous overexpression of enzymes of the lower part of glycolysis can enhance the fermentative capacity of *Saccharomyces cerevisiae*. *Yeast* **16**, 1325-34 (2000).
10. Schaaff, I., Heinisch, J. & Zimmermann, F.K. Overproduction of glycolytic enzymes in yeast. *Yeast* **5**, 285-90 (1989).
11. Roca, C., Haack, M.B. & Olsson, L. Engineering of carbon catabolite repression in recombinant xylose fermenting *Saccharomyces cerevisiae*. *Appl Microbiol Biotechnol* **63**, 578-83 (2004).
12. Gururajan, V.T., Gorwa-Grauslund, M.F., Hahn-Hagerdal, B., Pretorius, I.S. & Otero, R.R.C. A constitutive catabolite repression mutant of a recombinant *Saccharomyces cerevisiae* strain improves xylose consumption during fermentation. *Annals of Microbiology* **57**, 85-92 (2007).
13. Ostergaard, S., Olsson, L., Johnston, M. & Nielsen, J. Increasing galactose consumption by *Saccharomyces cerevisiae* through metabolic engineering of the GAL gene regulatory network. *Nat Biotechnol* **18**, 1283-6 (2000).
14. DeRisi, J.L., Iyer, V.R. & Brown, P.O. Exploring the metabolic and genetic control of gene expression on a genomic scale. *Science* **278**, 680-6 (1997).
15. Young, E.T., Dombek, K.M., Tachibana, C. & Ideker, T. Multiple pathways are co-regulated by the protein kinase Snf1 and the transcription factors Adr1 and Cat8. *J Biol Chem* **278**, 26146-58 (2003).
16. Daran-Lapujade, P. et al. Role of transcriptional regulation in controlling fluxes in central carbon metabolism of *Saccharomyces cerevisiae*. A chemostat culture study. *J Biol Chem* **279**, 9125-38 (2004).
17. Kim, J.H. & Johnston, M. Two glucose-sensing pathways converge on Rgt1 to regulate expression of glucose transporter genes in *Saccharomyces cerevisiae*. *J Biol Chem* **281**, 26144-9 (2006).
18. Polish, J.A., Kim, J.H. & Johnston, M. How the Rgt1 transcription factor of *Saccharomyces cerevisiae* is regulated by glucose. *Genetics* **169**, 583-94 (2005).
19. Kaniak, A., Xue, Z., Macool, D., Kim, J.H. & Johnston, M. Regulatory network connecting two glucose signal transduction pathways in *Saccharomyces cerevisiae*. *Eukaryot Cell* **3**, 221-31 (2004).

20. Ozcan, S., Dover, J., Rosenwald, A.G., Wolfl, S. & Johnston, M. Two glucose transporters in *Saccharomyces cerevisiae* are glucose sensors that generate a signal for induction of gene expression. *Proc Natl Acad Sci U S A* **93**, 12428-32 (1996).
21. Ozcan, S. & Johnston, M. Three different regulatory mechanisms enable yeast hexose transporter (HXT) genes to be induced by different levels of glucose. *Mol Cell Biol* **15**, 1564-72 (1995).
22. Winzeler, E.A. et al. Functional characterization of the *S. cerevisiae* genome by gene deletion and parallel analysis. *Science* **285**, 901-6 (1999).
23. Giaever, G. et al. Functional profiling of the *Saccharomyces cerevisiae* genome. *Nature* **418**, 387-91 (2002).
24. Kutykrishnan, S., Sabina, J., Langton, L.L., Johnston, M. & Brent, M.R. A quantitative model of glucose signaling in yeast reveals an incoherent feed forward loop leading to a specific, transient pulse of transcription. *Proc Natl Acad Sci U S A* **107**, 16743-8 (2010).
25. Loftus, B.J. et al. The genome of the basidiomycetous yeast and human pathogen *Cryptococcus neoformans*. *Science* **307**, 1321-4 (2005).
26. Tenney, A.E. et al. Gene prediction and verification in a compact genome with numerous small introns. *Genome Res* **14**, 2330-2335 (2004).
27. Usaite, R. et al. Reconstruction of the yeast Snf1 kinase regulatory network reveals its role as a global energy regulator. *Mol Syst Biol* **5**, 319 (2009).
28. Turcotte, B., Liang, X.B., Robert, F. & Soontornngun, N. Transcriptional regulation of nonfermentable carbon utilization in budding yeast. *FEMS Yeast Res* **10**, 2-13 (2010).
29. Soontornngun, N., Larochele, M., Drouin, S., Robert, F. & Turcotte, B. Regulation of gluconeogenesis in *Saccharomyces cerevisiae* is mediated by activator and repressor functions of Rds2. *Mol Cell Biol* **27**, 7895-905 (2007).
30. De Wever, V., Reiter, W., Ballarini, A., Ammerer, G. & Brocard, C. A dual role for PP1 in shaping the Msn2-dependent transcriptional response to glucose starvation. *Embo J* **24**, 4115-23 (2005).
31. Vyas, V.K., Kuchin, S. & Carlson, M. Interaction of the repressors Nrg1 and Nrg2 with the Snf1 protein kinase in *Saccharomyces cerevisiae*. *Genetics* **158**, 563-72 (2001).
32. Kuchin, S., Vyas, V.K. & Carlson, M. Snf1 protein kinase and the repressors Nrg1 and Nrg2 regulate FLO11, haploid invasive growth, and diploid pseudohyphal differentiation. *Mol Cell Biol* **22**, 3994-4000 (2002).
33. Toda, T. et al. Cloning and characterization of BCY1, a locus encoding a regulatory subunit of the cyclic AMP-dependent protein kinase in *Saccharomyces cerevisiae*. *Mol Cell Biol* **7**, 1371-7 (1987).
34. Varma, A. & Palsson, B.O. Metabolic Flux Balancing: Basic Concepts, Scientific and Practical Use. *Nat Biotech* **12**, 994-998 (1994).
35. Förster, J., Famili, I., Fu, P., Palsson, B.Ø. & Nielsen, J. Genome-Scale Reconstruction of the *Saccharomyces cerevisiae* Metabolic Network. *Genome Res* **13**, 244-253 (2003).
36. Duarte, N.C., Herrgård, M.J. & Palsson, B.Ø. Reconstruction and Validation of *Saccharomyces cerevisiae* iND750, a Fully Compartmentalized Genome-Scale Metabolic Model. *Genome Res* **14**, 1298-1309 (2004).
37. Kahn, B.B., Alquier, T., Carling, D. & Hardie, D.G. AMP-activated protein kinase: ancient energy gauge provides clues to modern understanding of metabolism. *Cell Metab* **1**, 15-25 (2005).
38. Patil, K.R. & Nielsen, J. Uncovering transcriptional regulation of metabolism by using metabolic network topology. *Proc Natl Acad Sci U S A* **102**, 2685-9 (2005).
39. Oliveira, A.P., Patil, K.R. & Nielsen, J. Architecture of transcriptional regulatory circuits is knitted over the topology of bio-molecular interaction networks. *BMC Syst Biol* **2**, 17 (2008).
40. Fendt, S.M. et al. Unraveling condition-dependent networks of transcription factors that control metabolic pathway activity in yeast. *Mol Syst Biol* **6**, 432 (2010).

41. Hector, R.E., Qureshi, N., Hughes, S.R. & Cotta, M.A. Expression of a heterologous xylose transporter in a *Saccharomyces cerevisiae* strain engineered to utilize xylose improves aerobic xylose consumption. *Appl Microbiol Biotechnol* **80**, 675-84 (2008).
42. Salusjarvi, L. et al. Regulation of xylose metabolism in recombinant *Saccharomyces cerevisiae*. *Microb Cell Fact* **7**, 18 (2008).
43. Trapnell, C., Pachter, L. & Salzberg, S.L. TopHat: discovering splice junctions with RNA-Seq. *Bioinformatics* **25**, 1105-11 (2009).
44. Trapnell, C. et al. Transcript assembly and quantification by RNA-Seq reveals unannotated transcripts and isoform switching during cell differentiation. *Nat Biotechnol* **28**, 511-5 (2010).
45. Bullard, J.H., Purdom, E., Hansen, K.D. & Dudoit, S. Evaluation of statistical methods for normalization and differential expression in mRNA-Seq experiments. *BMC Bioinformatics* **11**, 94 (2010).
46. Lo, K. & Gottardo, R. Flexible empirical Bayes models for differential gene expression. *Bioinformatics* **23**, 328-35 (2007).
47. Smyth, G.K. Linear models and empirical bayes methods for assessing differential expression in microarray experiments. *Stat Appl Genet Mol Biol* **3**, Article3 (2004).
48. Wishart, J.A., Hayes, A., Wardleworth, L., Zhang, N. & Oliver, S.G. Doxycycline, the drug used to control the tet-regulatable promoter system, has no effect on global gene expression in *Saccharomyces cerevisiae*. *Yeast* **22**, 565-9 (2005).
49. van den Berg, M.A. et al. The two acetyl-coenzyme A synthetases of *Saccharomyces cerevisiae* differ with respect to kinetic properties and transcriptional regulation. *J Biol Chem* **271**, 28953-9 (1996).
50. Ronen, M. & Botstein, D. Transcriptional response of steady-state yeast cultures to transient perturbations in carbon source. *Proc Natl Acad Sci U S A* **103**, 389-94 (2006).
51. Celenza, J.L. & Carlson, M. A yeast gene that is essential for release from glucose repression encodes a protein kinase. *Science* **233**, 1175-80 (1986).
52. Brumbaugh, J., Schleifenbaum, A., Gasch, A., Sattler, M. & Schultz, C. A dual parameter FRET probe for measuring PKC and PKA activity in living cells. *J Am Chem Soc* **128**, 24-5 (2006).
53. Cameron, S., Levin, L., Zoller, M. & Wigler, M. cAMP-independent control of sporulation, glycogen metabolism, and heat shock resistance in *S. cerevisiae*. *Cell* **53**, 555-66 (1988).
54. Gari, E., Piedrafita, L., Aldea, M. & Herrero, E. A set of vectors with a tetracycline-regulatable promoter system for modulated gene expression in *Saccharomyces cerevisiae*. *Yeast* **13**, 837-48 (1997).
55. Mnaimneh, S. et al. Exploration of essential gene functions via titratable promoter alleles. *Cell* **118**, 31-44 (2004).
56. Belle, A., Tanay, A., Bitincka, L., Shamir, R. & O'Shea, E.K. Quantification of protein half-lives in the budding yeast proteome. *Proc Natl Acad Sci U S A* **103**, 13004-9 (2006).
57. Lu, P., Vogel, C., Wang, R., Yao, X. & Marcotte, E.M. Absolute protein expression profiling estimates the relative contributions of transcriptional and translational regulation. *Nat Biotech* **25**, 117-124 (2007).
58. Shea, M.A. & Ackers, G.K. The OR control system of bacteriophage lambda. A physical-chemical model for gene regulation. *J Mol Biol* **181**, 211-30 (1985).
59. Gertz, J., Siggia, E.D. & Cohen, B.A. Analysis of combinatorial cis-regulation in synthetic and genomic promoters. *Nature* **457**, 215-8 (2009).
60. Gertz, J., Siggia, E.D. & Cohen, B.A. Analysis of combinatorial cis-regulation in synthetic and genomic promoters. *Nature* (2008).
61. Chen, C.C., Zhu, X.G. & Zhong, S. Selection of thermodynamic models for combinatorial control of multiple transcription factors in early differentiation of embryonic stem cells. *BMC Genomics* **9 Suppl 1**, S18 (2008).
62. Chen, C.C. & Zhong, S. Inferring gene regulatory networks by thermodynamic modeling. *BMC Genomics* **9 Suppl 2**, S19 (2008).



63. Lubliner, S. & Segal, E. Modeling interactions between adjacent nucleosomes improves genome-wide predictions of nucleosome occupancy. *Bioinformatics* **25**, i348-55 (2009).
64. Raveh-Sadka, T., Levo, M. & Segal, E. Incorporating nucleosomes into thermodynamic models of transcription regulation. *Genome Res* **19**, 1480-96 (2009).
65. Segal, E., Raveh-Sadka, T., Schroeder, M., Unnerstall, U. & Gaul, U. Predicting expression patterns from regulatory sequence in *Drosophila* segmentation. *Nature* **451**, 535-40 (2008).
66. Kertesz, M., Iovino, N., Unnerstall, U., Gaul, U. & Segal, E. The role of site accessibility in microRNA target recognition. *Nat Genet* **39**, 1278-84 (2007).
67. Haynes, B.C., Kramer, M.H. & Brent, M.R. Resolving the structure of transcriptional networks using signal attenuation. **In review**(2011).
68. Orth, J.D., Thiele, I. & Palsson, B.O. What is flux balance analysis? *Nat Biotechnol* **28**, 245-8 (2010).
69. Shlomi, T., Eisenberg, Y., Sharan, R. & Ruppin, E. A genome-scale computational study of the interplay between transcriptional regulation and metabolism. *Mol Syst Biol* **3**, 101 (2007).
70. Raman, K. & Chandra, N. Flux balance analysis of biological systems: applications and challenges. *Brief Bioinform* **10**, 435-49 (2009).
71. Madar, A., Greenfield, A., Ostrer, H., Vanden-Eijnden, E. & Bonneau, R. The Inferelator 2.0: a scalable framework for reconstruction of dynamic regulatory network models. *Conf Proc IEEE Eng Med Biol Soc* **2009**, 5448-51 (2009).
72. Bonneau, R. et al. The Inferelator: an algorithm for learning parsimonious regulatory networks from systems-biology data sets de novo. *Genome Biol* **7**, R36 (2006).